SWIFT-XRT-CALDB-11

Release Date: May 9th, 2008

Prepared by: Olivier Godet[1], Andrew P. Beardmore[1], Sergio Campana[2], Giancarlo Cusumano[3]

Date revised: May 7th, 2008

Revision: 1.0

Revised by: Olivier Godet

[1] Leicester, [2] INAF-OAB, [3] INAF-IASF Palermo

SWIFT XRT CALDB RELEASE NOTE
SWIFT-XRT-CALDB-11: Response matrices and Ancillary Response Files

Table 1: Component files:

Filename	Mode	Grade	Substrate* voltage (V)	Date
swxwt0to2s0_20010101v011.rmf swxwt0to2s6_20010101v011.rmf swxwt0to2s0_20010101v011.arf swxwt0to2s6_20010101v011.arf	WT	0-2	0 6 0 6	09/05/08
swxwt0s0_20010101v011.rmf swxwt0s6_20010101v011.rmf swxwt0s0_20010101v011.arf swxwt0s6_20010101v011.arf	WT	0	0 6 0 6	09/05/08
swxpc0to12s0_20010101v011.rmf swxpc0to12s6_20010101v011.rmf swxpc0to12s0_20010101v011.arf swxpc0to12s6_20010101v011.arf	PC	0-12	0 6 0 6	09/05/08
swxpc0s0_20010101v011.rmf swxpc0s6_20010101v011.rmf swxpc0s0_20010101v011.arf swxpc0s6_20010101v011.arf	PC	0	0 6 0 6	09/05/08
swxpd0to5_20010101v007.rmf swxpd0to5_20010101v003.arf	LRPD	0-5	0	04/05/05 07/04/05
swxpd0to2_20010101v007.rmf swxpd0to2_20010101v003.arf	LRPD	0-2	0	04/05/05 07/04/05
swxpd0_20010101v007.rmf swxpd0_20010101v003.arf	LRPD	0	0	04/05/05 07/04/05

*The substrate voltage was permanently raised from $V_{ss} = 0\,\mathrm{V}$ to $V_{ss} = 6\,\mathrm{V}$ on 2007 August 30 (see Section 4).

1 Scope of Document

This note describes the release of the *Swift* XRT redistribution matrix (RMF v011) and ancillary response (ARF v011) files (see Table 1). Files are released for each working XRT mode (Photon Counting, PC, Window Timing, WT) and two different grade selections for each mode.[1] In this release, the WT RMFs/ARFs and PC mode ARFS are newly computed files, while the PC RMFs are the same as those issued in the previous releases SWIFT-XRT-CALDB-09/10, though the file names have been changed in order to provide a uniform naming scheme.

On 2007 August 30 (at 14:28UT), the CCD substrate voltage was raised from $V_{ss} = 0\,\mathrm{V}$ to $V_{ss} = 6\,\mathrm{V}$. The change was made in order to reduce the thermally induced dark current in the CCD, which allows the XRT to collect useful science data at slightly higher temperatures (3 to 4 C) than was possible before the change. The change in substrate voltage has made it necessary to release two sets of RMF/ARF files, now distinguished by the characters 's0' and 's6' in their file names. At the moment the $V_{ss} = 6\,\mathrm{V}$ files are placeholders and identical to the 0V files. A future release will made for the 6 V files, however the calibration changes are expected to be small (see section 4).

The XRT effective area is made by three main components: the mirror effective area, the CCD quantum efficiency (QE) and the filter transmission. The QE is included directly in the redistribution matrix. The ARF files contain the mirror effective area, the filter transmission, as well as the vignetting correction and the Point Spread Function (PSF) correction (which depends on the source location and of the size of the extraction region, as well as on defects on the CCD). Here we report on the CALDB RMF and ARF files which represent the effective area of the telescope for a nominal on-axis observation (no vignetting correction) and for an infinite region of interest (no correction for PSF losses). RMF files do not include the PSF correction and do not depend on the source position on the detector. The CCD soft energy response is sufficiently uniform within the central 200x200 pixels (see e.g. previous RMF release notes), therefore there is just one RMF file per mode and grade selection. The ARF files, instead, need vignetting and PSF corrections and, therefore, need to be built for each observation. To produce the observation-specific ARF files, the XRTMKARF task (XRTDAS-HEADAS software) has been developed. This task corrects the nominal ARF file for the vignetting and, optionally (psfflag=yes), for PSF losses. This task includes corrections for CCD defects with the inclusion of an exposure map automatically generated by the data analysis pipeline (expofile=filename.img). The adopted calibration method implies that we include the residual correction of the CCD quantum efficiency in the CALDB ARF files, accounting for why the nominal ARF files are different for different grade selection.

2 RMF generation

The Response Matrix Files (RMFs) are created by a Monte-Carlo simulation code (Godet et al. 2007, SPIE, 6686, 6686OA1 ; Osborne et al. 2005, SPIE 5859 340). This code models: transmission of the incident X-rays through the CCD electrode structure; photo-absorption in the active layers of the device; charge cloud generation, transportation and spreading; silicon fluorescence and its associated escape peak; surface loss effects; mapping of the resultant charge-cloud to the detector pixel array; charge transfer efficiency; addition of electronic read-out noise; event thresholding and classification according to the specific mode of operation.

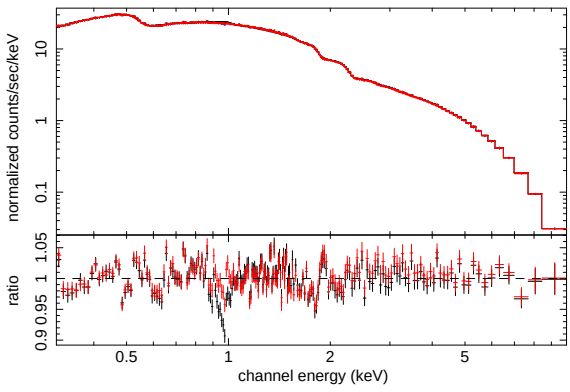

Figure 1: Fits of Mkn421 in WT mode showing the improvement in the RMF redistribution in the 0.9-1 keV energy band obtained with the v011 RMF (v011: red grade 0-2 - v010: black grade 0-2). Note that we used the v011 ARF to perform the fits (see Section 3). The spectrum contains more than 10^6 counts.

In the release SWIFT-XRT-CALDB-08, in orbit observations of the soft calibration sources were used to refine the surface loss function in order to better match the spectral redistribution at low energies. While for heavily absorbed sources, the parameterisation of the redistribution of high energy X-rays down to low energies was improved for both

[1] Files for the Low Rate PhotoDiode mode were not updated after the XRT CCD was damaged by a micro-meteorite strike on 27th May 2005, resulting in the loss of this operational mode. For this mode the older (rmf v007 and arf v003) response can be used. We have not updated the PC response for grade 0-4 either, as, in practice, it is rarely used. Testing has been carried out extensively on WT grade 0, 0-2 and PC grade 0, 0-12.

PC and WT modes (using SNR G21.5, SGR 1900+14 & NGC 7172 for PC, and GROJ1655-40, 4U1608-52, XTE J1701-462 & GX17+2 for WT) by including a correction to the loss-shelf (see the release note SWIFT-XRT-CALDB-10). For PC mode, a new charge-cloud spreading model was implemented following the theory of Pavlov & Nousek (1999 NIMA 428 348), which better accounts for sub-threshold losses seen in the more energetic multi-pixel events (see the release SWIFT-XRT-CALDB-10).

Specifically, for this release (SWIFT-XRT-CALDB-11), a slight change in the loss function parameters between 1 keV and 2 keV in WT mode was implemented to suppress the 10% residuals around 0.9-1 keV only visible in high statistical spectra (see Figure 1). For both modes, updated Charge Transfer Inefficiency (CTI) values were used, which are more appropriate for the CTI degradation suffered in orbit during the middle of 2006.

3 ARF generation

In order to model the overall XRT response we used the latest RMF matrices (hereby released) and fine tuned the ARF files on X-ray spectra from different celestial sources. Following the previous release, we adopted a multi-source approach, with the sources having different spectral characteristics, to improve the calibration. We did this by comparing the spectral parameters and absolute flux of several calibration sources with spectra taken by XMM-Newton (primarily the EPIC-MOS) in order to improve the absolute flux determination in both WT and PC modes, as well as use the same source in WT and PC, wherever possible, to ensure consistency between the two.

3.1 Windowed Timing mode

First of all, we became fully aware that the off-pulse spectrum of the Crab nebula is still slightly piled-up, so to improve the XRT response description we did not use this source to calibrate the WT mode. Another step forward came with the opportunity to dynamically correct for possible bias offsets in WT mode observations within xrtpipeline using the wtbiasmode=M20P option (which, since build 2.6 of the *Swift* software tools, is now the default). This option computes the bias difference between the on-ground estimated bias median from the last 20 pixels data telemetered with every frame, and the median of the last 20 pixels in the related bias row (which was subtracted automatically on-board). This improved, substantially, the description of the WT mode data and led us to be confident in the reality of the absorption-like feature observed in a number of spectra at low energies (oxygen edge). In the releases SWIFT-XRT-CALDB-08/10, we made an ad-hoc correction to the WT ARF around the oxygen edge. Further investigation showed that the absorption-like feature seen in WT mode is likely due to an energy offset between the PC and WT energy scales. We estimated the offset value to be 17.6 eV by comparing PC and WT spectra of line sources such as the SNR E0102-72.3 and Cas A (see Figure 2). The introduction of an offset of 17.6 eV in the WT gain file showed that the ad-hoc correction around the oxygen edge in WT mode are no longer necessary (see Figs. 1 and 3).

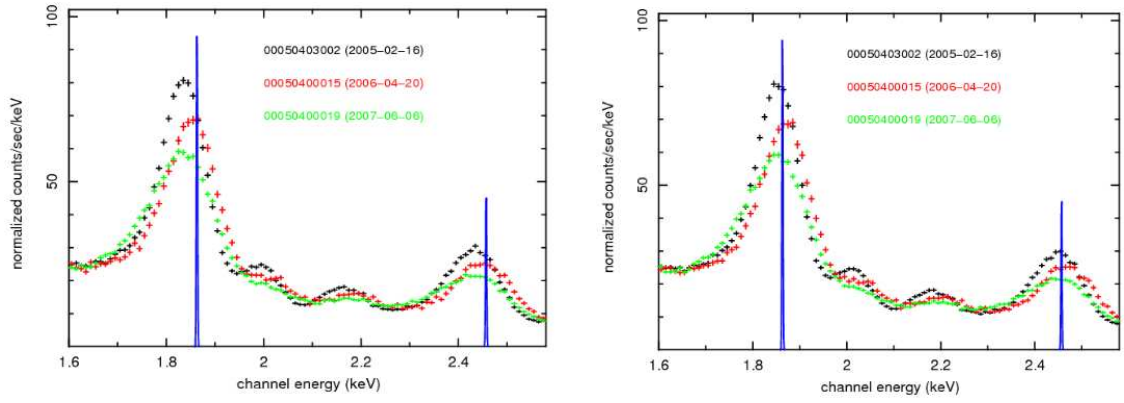

Figure 2: Spectra of the entire SNR Cas A in WT mode at different epochs. The blue line indicates the expected energy centroid of the Si and S Kα lines. Left - Data processed using the v007 gain file. Right - Data processed using the v008 WT gain file including an offset of 17.6 eV.

The first improvement to the ARF at low energies came by including the detailed medium-thickness filter transmission curve from the XMM-Newton MOS detector. This is identical in composition and thickness to the *Swift* XRT filter, so that differences between the two are expected to be negligible. This new filter curve introduces a number of fine structure features in the O-edge (0.54 keV) and Al-edge (1.56 keV).

In the releases SWIFT-XRT-CALDB-07/10, an observation of the isolated neutron star RXJ1856-37 was used to normalise the effective area at low energies (< 2 keV). Using the model of Beuermann et al. (2006 A&A 458 541, derived from Chandra LETG), which is essentially a 63 eV black-body in the XRT band, we found that the soft band flux is also accurate to approximately 5%. Further investigation showed that the rescaling down of the ARF below

2 keV could be naturally accounted for by a reduction of the open electrode area of the CCD-22 geometry (by less than 10%) assumed in the CCD response model producing the RMFs. We used, in this release, this new modelling to define the shape of the WT ARFs below 2 keV. The new sets of WT ARFs v011 give results similar to the WT ARFs v010.

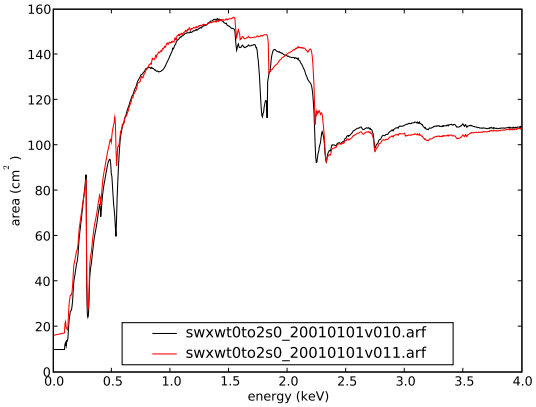

Figure 3: Comparison of the ARF in WT mode (v011: red grade 0-2 - v010: black grade 0-2). Note that the ad-hoc corrections around the oxygen edge and at 0.9 keV are no longer needed since we introduced an offset of 17.6 eV with respect to the v007 WT gain file and since we produced the v011 RMFs, respectively.

We then used as a primary calibrator for WT mode two observations of Mkn 421. The first (obsid 00030352011, 33ks exposure with 1.3×10^6 counts) was used to apply ad-hoc corrections to residuals around the Au edges (2.2-3.0 keV) and the Si-edge (1.84 keV) after processing the data with the v008 WT gain file including an offset of 17.6 eV. The second observation (obsid 00030352017, 4.4ks exposure), which was taken simultaneously with the XMM-Newton EPIC cameras (in timing mode), was used to verify that the derived spectral fit parameters were acceptable. Fitting an absorbed, continuously bending power-law model to these data (see Figure 1) we obtained the following results:

	Photon index	Bending parameter	Obs. Flux (0.3-10 keV) ($\times 10^{-10}$ erg cm^{-2} s^{-1})
MOS1	2.365 ± 0.015	-0.42 ± 0.03	4.48
WT g0-2	2.304 ± 0.011	-0.41 ± 0.03	4.39

Table 2: Results obtained when fitting XRT WT and XMM MOS1 timing mode spectra from Mkn 421 with a continuously bending power-law model.

Additionally, observations of the quasar 3c273 (obsid 00050900003/4/5/6/7), taken simultaneously with XMM and RXTE, were compared in order to verify the global effective area and spectral parameters (modelled by an absorbed power-law plus 2 zbbody and a fixed N_H-value of 1.79×10^{20} cm^{-2}):

Table 3: Cross-calibration results obtained on 3C273 comparing XRT WT, XMM and RXTE datasets.

	Photon index	Blackbody temp. kT_1 (keV)	Blackbody temp. kT_2 (keV)	Obs. Flux (0.3-10 keV) ($\times 10^{-10}$ erg cm^{-2} s^{-1})	Obs. Flux (2-10 keV) ($\times 10^{-10}$ erg cm^{-2} s^{-1})
PN	1.646 ± 0.011	0.074 ± 0.003	0.186 ± 0.011	1.47 ± 0.01	0.85 ± 0.01
MOS1	1.500 ± 0.028	0.089 ± 0.004	0.304 ± 0.015	1.53 ± 0.01	0.95 ± 0.01
MOS2	1.533 ± 0.025	0.072 ± 0.004	0.266 ± 0.014	1.53 ± 0.01	0.93 ± 0.01
WT g0-2	1.57 ± 0.04	0.050 ± 0.030	0.136 ± 0.060	1.61 ± 0.03	1.02 ± 0.02
WT g0	1.56 ± 0.04	0.046 ± 0.030	0.129 ± 0.090	$1.65^{+0.03}_{-0.04}$	1.02 ± 0.03
XTE	1.62 ± 0.03	-	-	-	1.02 ± 0.01

The above results (see figure 4) show that the XRT WT grade 0-2 and grade 0 fluxes are accurate to 5% compared to the MOS, 10% compared to the PN and are in agreement with XTE.

In conclusion, we recommend to fit the XRT WT spectra in the 0.3-10 keV energy range with these updated XRT responses files. A systematic error less than 3% is needed for high statistical spectra.

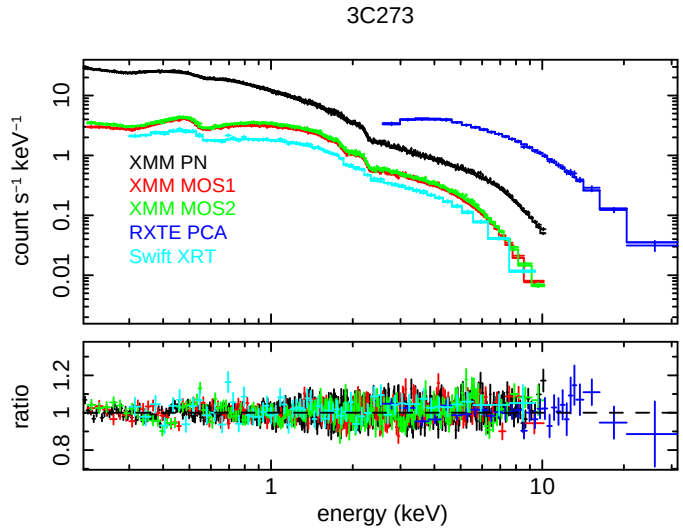

Figure 4: Simultaneous XMM-Newton, *Swift* and XTE observations of 3c273 showing the PN (black), MOS1 (red), MOS2 (green), XTE (blue) and XRT WT g0-2 (cyan) fit. Note that the levels of residuals in the XRT spectrum are similar to those obtained with the XMM-EPIC instruments.

3.2 Photon Counting mode

The PC mode grade 0 and grade 0–12 RMFs were not modified for this release and are the same files found in v009/010 but renamed to v011 in order to reflect a common naming scheme. However, a new task XRTPCBIAS was released with build v2.7 of the *Swift* software tools which dynamically corrects the PC bias, if required, using the local bias estimated from the corner pixels of single-pixel events. The effect of the correction is most notable around the instrumental edges of Oxygen, Silicon and Gold for sources with long exposures — hence for good statistical quality data. Ad-hoc changes had been made around the edges in the previous release, but because of XRTPCBIAS, and together with the improved WT ARF files (section 3.1), we revisited the PC effective area calibration.

The global PC effective area was calibrated on the BL Lac object PKS2155–304, using an observation (obsid 00030795028, taken 2007-04-22) which was simultaneous with XMM-Newton, while the residuals around the Si and Au edge were checked using 147ks of data (50k counts) accumulated on 3C279 in 2006 (see figure 5). For PC grade 0-12, by starting with the WT grade 0–2 ARF we found it only had to be scaled below the Si edge (1.84 keV) by 15% to give a good match with the data, while above this energy the area was consistent with the WT grade 0-2 area, as expected for these grade selections. For PC grade 0, the area profile from the v010 release was retained above the main Au edge at 2.2 keV. Below this edge, the new WT grade 0 ARF profile was used, after rescaling to the same level as the v010 grade 0 ARF. The cause of the discrepancy between the observed and expected PC grade 0 QE, and the PC grade 0–12 QE below 1.84 keV, is still under investigation. Figure 6 shows a comparison of the newly created PC ARFs for the v011 release with the previous v010 release.

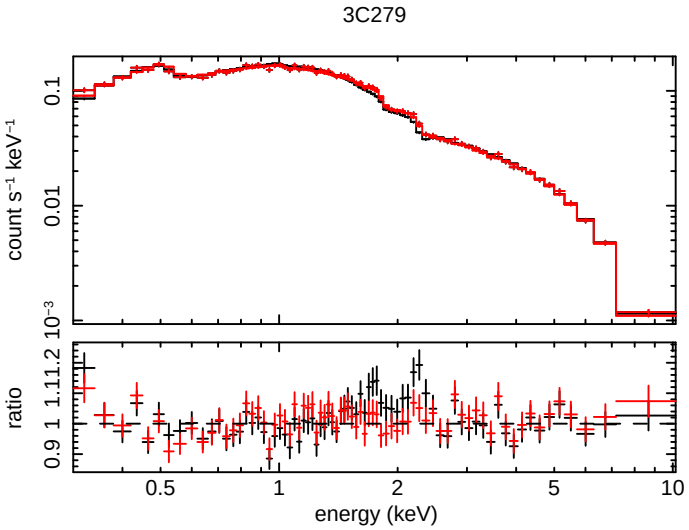

Figure 5: Comparison of spectral fits for the new grade 0–12 PC mode ARF for v011 (red) with v010 (black) when fit to 147ks of data taken on 3C279. V011 shows improved residuals around the Si and Au edges. The spectrum contains 50k counts.

As with WT mode, the primary low energy calibrator below 1 keV was the neutron star RXJ1856–37. Using the previously described model for this source (see section 3.1), which is 63 eV black-body, and allowing just the

normalisations to vary, we obtain soft band fluxes which agree to within 2% of the expected model using the new PC v011 ARFs, compared with 6% for the previous release.

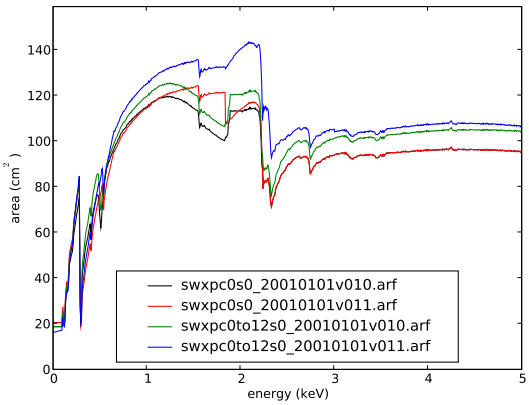

Figure 6: Comparison of the new v011 PC mode ARFs (grade 0-12, blue; grade 0, red) with v010 (grade 0–12, green; grade 0, black). The black and red curves are identical above 2.2 keV.

The medium and higher area energy calibration was verified on the galaxy cluster PKS0745–19 and the SNR G21.5 in comparison with results from XMM. The following table lists the results of fitting an absorbed power-law, or thermal Mekal, model to PKS2155–304, PKS0745–19 [2] and SNR G21.5 [2] and includes the XMM results for comparison.

Table 4: PC mode cross-calibration comparison for the new v011 ARFs.

	N_H (10^{22} cm^{-2})	Γ or kT	Flux (0.3-10 keV) ($\times 10^{-11}$ erg cm^{-2} s^{-1})
PKS2155-304			
PN	0.0124 (fixed)	2.676 ± 0.007	15.88 ± 0.06
MOS1		2.59 ± 0.01	14.27 ± 0.09
MOS2		2.56 ± 0.01	15.21 ± 0.10
PC g0-12		2.54 ± 0.03	14.94 ± 0.22
PC g0		2.52 ± 0.03	15.12 ± 0.26
SNR G21.5			
PN	3.028 ± 0.050	1.774 ± 0.020	4.08 ± 0.03
MOS1	3.188 ± 0.068	1.778 ± 0.031	4.45 ± 0.05
MOS2	3.227 ± 0.074	1.826 ± 0.033	4.59 ± 0.06
PC g0-12	3.21 ± 0.17	1.782 ± 0.072	4.53 ± 0.12
PC g0	3.34 ± 0.19	1.831 ± 0.086	4.72 ± 0.15
PKS0745-19			
MOS1	0.52 ± 0.01	6.55 ± 0.19	4.49 ± 0.05
PC g0-12	0.54 ± 0.01	6.60 ± 0.22	4.81 ± 0.05
PC g0	0.55 ± 0.01	6.54 ± 0.25	5.11 ± 0.06

The table shows the new ARFs produce a good agreement between grades 0 and 0–12 and give comparable results to XMM-Newton for a broad range of spectral types. The statistical uncertainty in the final v011 RMF/ARF combination in PC mode is estimated at 3% level in the 0.3-10 keV energy range.

4 Current limitations and future prospects

Our current understanding of the XRT response at $V_{ss} = 0$ V implies a systematic uncertainty less than 3% in WT mode and less than 3% in PC mode in the 0.3-10 keV energy band (the recommended band to be used) and better than 10% in absolute flux. The following considerations apply to both WT and PC mode observations.

[2] Custom extended source ARF files were built for the PKS0745–19 and SNR G21.5 XRT observations, taking into account their respective exposure maps, as XRTMKARF does not presently handle the generation of ARFs for extended sources.

- While the loss-shelf has been significantly improved, and with it the modelling of the redistribution for heavily absorbed sources, there is still scope for future enhancements in this area.
- We observe a degradation of the energy resolution, from 146 eV at 5.9 keV in February 2005 to 210 eV in March 2007 (based on the on-board corner sources) due to the build-up of charge traps on the CCD due to radiation and high-energy proton damage. The broadening of the line is due to the energy scale shifting effect of traps in the pixels through which the charge has to be transported. Prospects to implement a column by column description of the bias correction in the ground software are under investigation for PC and WT data after June 2007 (see Fig. 7). In parallel, response matrices with a broadened kernel in WT mode have been developed for data taken before June 2007 and are under testing at the moment. These RMFs take into account the line broadening due to trap effect.

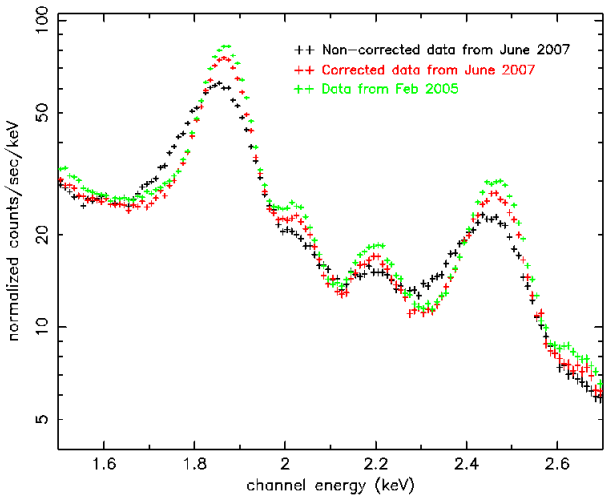

Figure 7: WT grade 0-2 spectra of the SNR Cas A (black crosses: from June 2007 data - red crosses: the June 2007 data are corrected from the effect of the charge traps by correcting the bias column by column - green crosses: from February 2005 data. The energy resolution (FWHM) of the Si Kα lines increases from 105 eV in February 2005 to about 131 eV in June 2007 (from non-corrected data). The degradation of the FHWM over time is due to an increase of the charge traps on the CCD over time.

- The build-up of charge traps on the CCD results in a loss of events at low-energy below the on-board energy threshold as shown in Fig. 8. From this spectrum, we noticed a decrease of the flux level by 15-20% from February 2005 to June 2007. The experimental WT RMFs with a broadened kernel presently under testing allow to retrieve the correct constant factor since they take into account the fraction of events lost below the on-board threshold. So, we recommend to be cautious about the flux level when fitting soft sources until adequate response files are released.

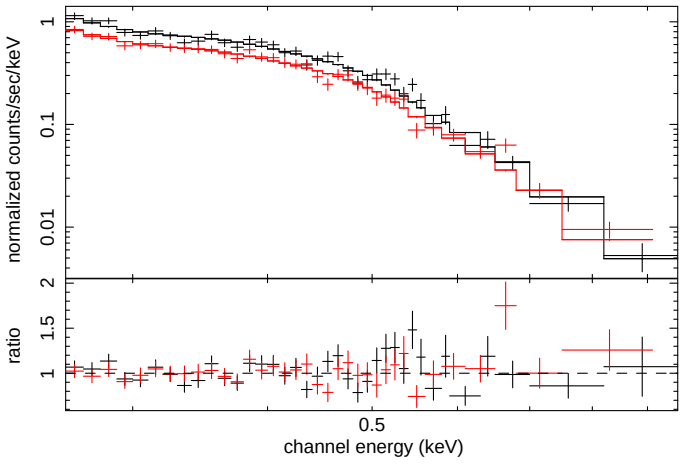

Figure 8: Evolution of the PC grade 0 spectrum of the soft neutron star RX J1856.4-3754 over time: (red) data from February 2005 (a constant factor of 0.96±0.03) and (black) data from June 2007 (a constant factor of 0.76 ± 0.03). The spectra were fitted using the v011 RMF. Note that only orbits of data when the source was not on the bad columns were used to make the spectra. When using the v011 WT g0 RMF, a similar evolution is also observed in WT mode with a constant factor of 0.96 ± 0.03 from February 2005 data and 0.80 ± 0.03 from June 2007. The decrease of the spectral evolution is due to the build-up of charge traps on the CCD over time so that a fraction of low-energy events are lost below the on-board event threshold.

Substrate Voltage Change

The loss of the active cooling causes the XRT to operate at higher than expected temperatures; this generates significant thermally-induced noise appearing as low energy events. Raising the substrate voltage as described in Osborne et al. 2005 (SPIE, 5859, 340) enables a reduction of this noise and the use of lower energy X-ray events, since the volume of Silicon in which carriers are generated is reduced. So, for these reasons the substrate voltage was permanently raised from $V_{ss} = 0\,\mathrm{V}$ to $V_{ss} = 6\,\mathrm{V}$ on 2007 August 30. The raise of the substrate voltage resulted in a slight decrease of the QE at high energy ($\sim 7\%$ at 6 keV as measured using on-board calibration sources). Fitting a model consisting of TBabs*powerlaw to the PC g0-12 spectra of the SNR G21.5 at $V_{ss} = 0$ and $6\,\mathrm{V}$ (both spectra contain over 10^4 counts) using the v010 PC response files, with the abundances fixed to those given by Wilms et al. (2000, ApJ, 542, 914), gives the following results:

	N_H (10^{22} cm^{-2})	Photon index
$V_{ss} = 0\,\mathrm{V}$	$3.24^{+0.19}_{-0.18}$	1.89 ± 0.08
$V_{ss} = 6\,\mathrm{V}$	$3.17^{+0.15}_{-0.14}$	1.87 ± 0.07

Both spectra were obtained using the data from the 40" core of the remnant. The slight reduction of the high-energy QE will be hardly noticeable for most sources observed in PC mode as shown above. The impact of the raise of the substrate voltage will be more noticeable in WT observations only for high statistical spectra with more than 10^5 counts. Even if the change in the QE is minimal, new response files at $V_{ss} = 6\,\mathrm{V}$ need to be generated. In the meantime, we recommend the use of the current release of the response files.